

Supplemental Figures and Legends

Figure S1: AC dynamics and function as an MTOC. Related to Figures 1 and 2.

(A) UL99-eGFP labels TGN46-positive regions early in infection. NHDFs were infected with TB40/E-UL99-eGFP at MOI 0.5. Cells were fixed at the indicated times and stained for GFP and TGN46. Nuclei were stained with Hoechst. The kinetics of Golgi remodeling into an AC and the localization pattern of UL99-eGFP with TGN46 are in line with prior fixed imaging studies, validating UL99-eGFP as a means to label the AC from its earliest stages of formation for live cell imaging. (B) Nucleating material localizes to Golgi-based sites throughout the AC (related to Figure 2A). NHDFs were infected with AD169 at MOI 3 for 3d. Fixed cells were stained for pericentrin and TGN46. (C-D) HCMV induces the formation of a subpopulation of MTs containing acetylated tubulin. NHDFs were mock infected or infected with TB40/E at MOI 1 for 5d. (C) Cells were fixed and stained for detyrosinated (Glu) or acetylated tubulin, along with TGN46. Typical examples of detyrosinated and acetylated tubulin networks are shown. White arrows point to singular asters of acetylated tubulin emanating from centrosomes in uninfected cells. Note that uninfected or infected NHDFs do not contain significant levels of detyrosinated MTs. 293 cells served as a positive control for detection of detyrosinated MTs. (D) Cells were fixed and stained for acetylated tubulin and TGN46. Nuclei were stained with Hoechst. Examples of acetylated networks found in uninfected or infected cells are shown. White arrows point to singular asters of acetylated tubulin emanating from centrosomes in uninfected cells. Right: The number of cells containing acetylated MT networks was quantified. Acetylated MTs were categorized as low,

medium or high. For examples of each category see left panels and Figure 5A-B. n = as indicated.

Figure S2: Effects of HCMV infection on the levels and localization of EB family members. Related to Figure 3.

(A) NHDFs were infected with laboratory (AD169) or clinical (FIX) strains of HCMV at MOI 3 for the indicated time in d.p.i. Cell lysates were analyzed by WB using the indicated antibodies. Although different HCMV strains have different kinetics of early gene expression and replication, in all three HCMV strains tested the increase in EB protein abundance coincided with the expression of IE2, but not IE1. (B) IE1/2 siRNAs do not indirectly affect EB protein levels in mock-infected cells. NHDFs were treated with control or IE1/2 siRNA for 3d. Cell lysates were analyzed by WB using the indicated antibodies. (C-E) Localization of EB proteins in HCMV-infected cells. Blue arrows point to examples of EB1 or EB3 comets at MT plus-ends, and the weaker plus-end accumulation of EB2. NHDFs were mock infected or infected with TB40/E at MOI 3 for 5d. Samples were stained for EB1 (C), EB2 (D) or EB3 (E). In addition, depending on antibody compatibility with each EB, samples were co-stained with antibodies against either tyrosinated-tubulin or α -tubulin to detect MTs, and HCMV gB or TGN46 to label the AC. Nuclei were stained with Hoechst. Right Panels: Zoomed images showing the plus-end distribution of EB1 and EB3, and the MT lattice localization of EB2. (F) EB3 localizes at and around γ -tubulin-positive regions of the AC. NHDFs were infected with TB40/E at MOI 3 for 5d. Fixed cells were stained for γ -tubulin and EB3. Nuclei were

stained with Hoechst. Samples were imaged using confocal microscopy. A representative maximum projection through the AC is shown.

Figure S3: Characterization of HEBTRON. Related to Figure 6 and 7.

(A) The DARTS method for drug target identification. Recombinant full-length human EB3 was incubated with or without the indicated peptides targeting EB1 or EB3, and digested with thermolysin. The products of digests were analyzed by WB for EB3. (B-C) Control experiments related to the results in Figure 6A. ITC of EB3 C-terminus (200-281aa) alone (B) and HEBTRON alone (C). This data shows that changes in heat during formation of the EB3-HEBTRON complex were not the result of dilution of the protein or peptide alone. (D) The effects of HEBTRON compared with vehicle (DMSO) on eGFP-CLIP170 tracking behavior. NHDFs expressing eGFP-CLIP170 were treated with DMSO or 25 μ M HEBTRON followed by infection with TB40/E at MOI 0.5 for 5d. Different frames from time-lapse sequences were color-coded and overlaid to generate FireRainbow images of eGFP-CLIP170 movement. A FireRainbow map is provided beneath. Right: Line-scan analysis of eGFP-CLIP170 intensity and distribution in DMSO or HEBTRON-treated cells. n = 5 (125 MT linescans per condition), bars = s.e.m. Note, HEBTRON does not affect MT dynamics or recruitment of CLIP170 to MT tips, similar to EB3 depletion in Figure 4F-G. (E-G) HEBTRON does not affect Vaccinia Virus replication or spread. NHDFs were treated with DMSO or 25 μ M HEBTRON, MutN or MutN-MutC, followed by infection with Vaccinia Virus expressing a GFP-tagged B5 protein (VacV-B5-GFP) at MOI 0.01 for 36h. (E) Phase and fluorescence images of plaques were acquired. 50 pixel background subtraction was performed using Fiji to

reduce autofluorescence from plate. Representative images are shown. (F) The sizes of VacV-B5-GFP plaques formed under each condition were measured using Fiji. $n = 3$ biological replicates (>53 plaques), bars = s.e.m. ns= not significant. (G) Cultures were lysed and analyzed by WB using a pan-VacV antibody that detects viral structural proteins. Asterisks highlight a non-specific host protein also detected in mock-infected samples. (H) HEBTRON does not affect EB3 localization to the AC. NHDFs were treated with DMSO or 25 μ M HEBTRON followed by infection with TB40/E at MOI 1 for 5d. Fixed samples were stained for EB3 and gB. Nuclei were stained with Hoechst. No difference in EB3 localization to the AC could be observed between DMSO or HEBTRON-treated cultures. Representative images are shown.

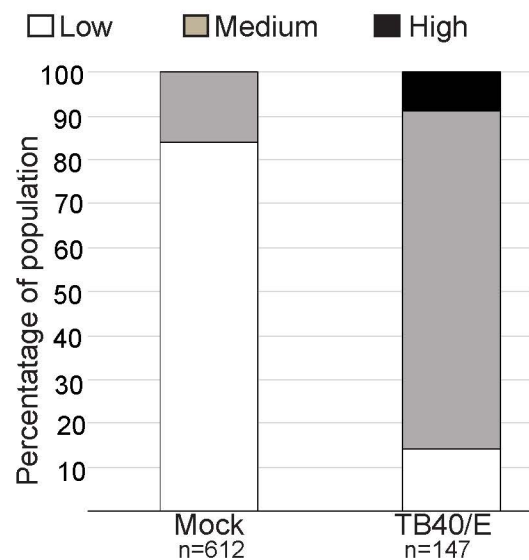
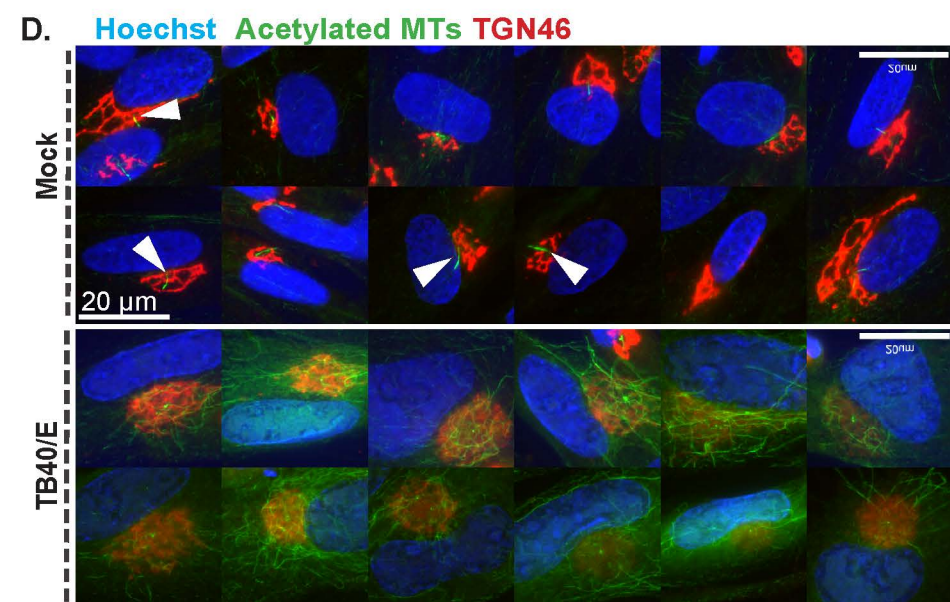
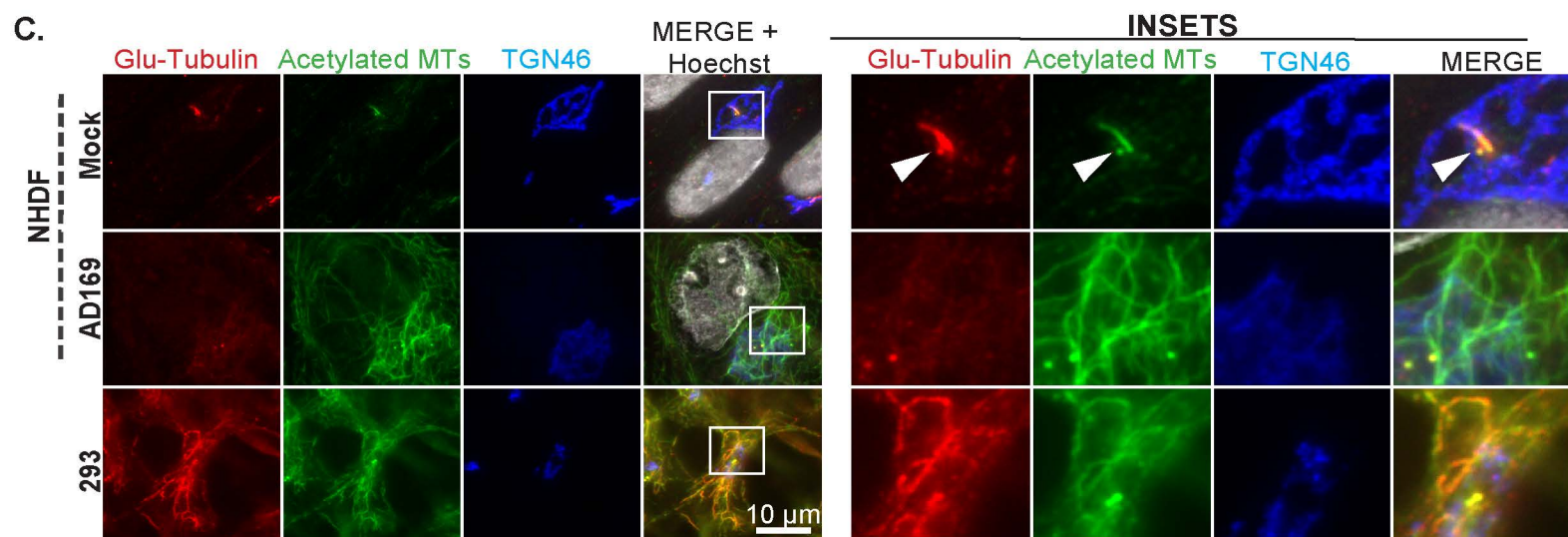
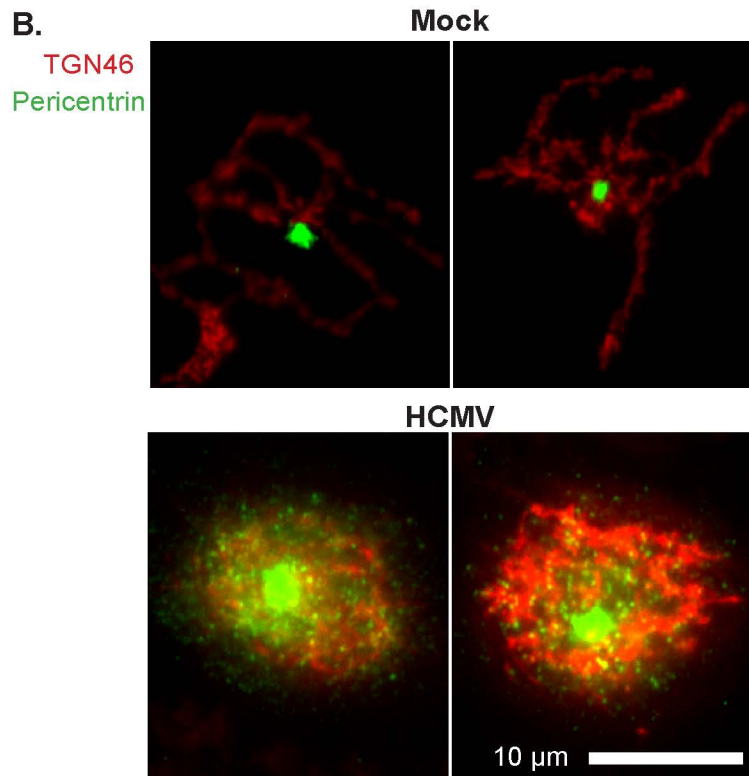
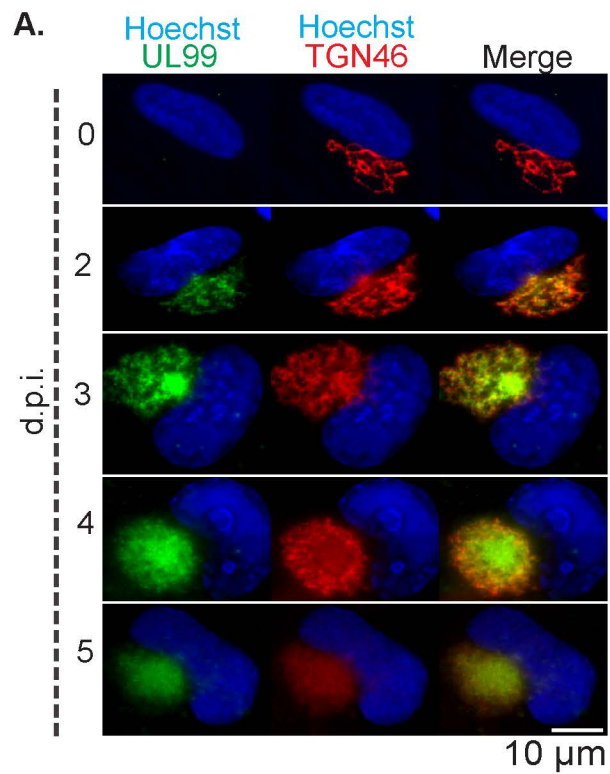
Figure S4. Displacement of SxIP-interacting proteins by HEBTRON and the role of EB3 in non-centrosomal MT formation in HCMV-infected cells. Related to Figure 7.

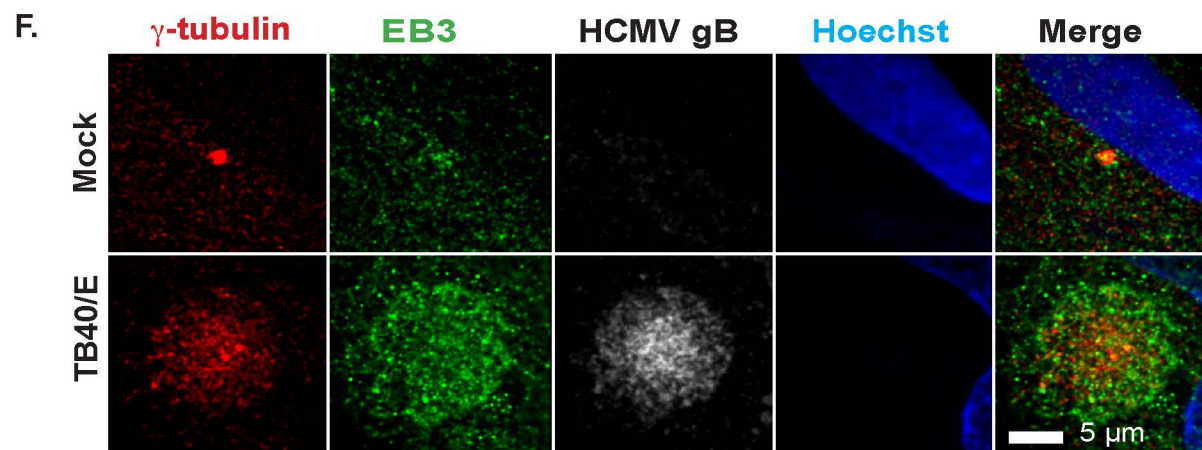
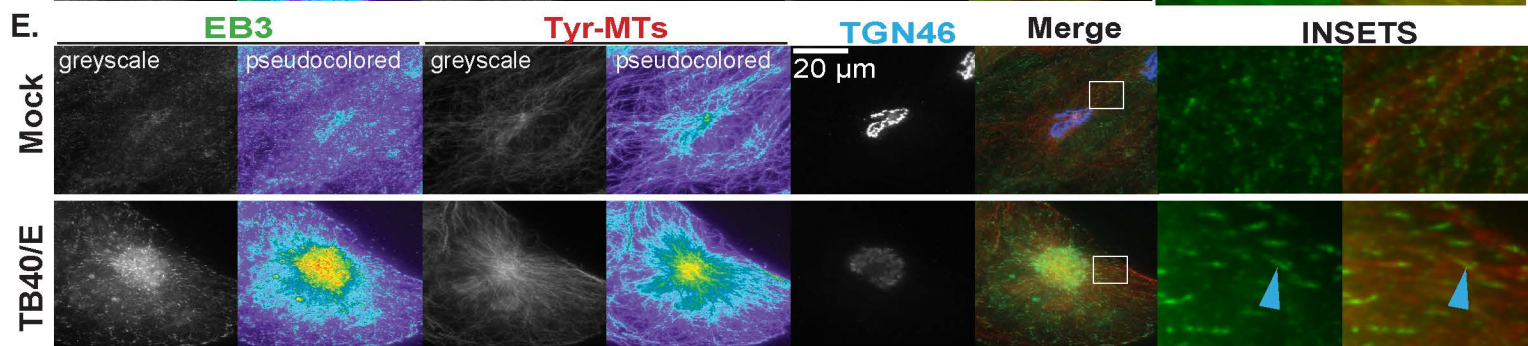
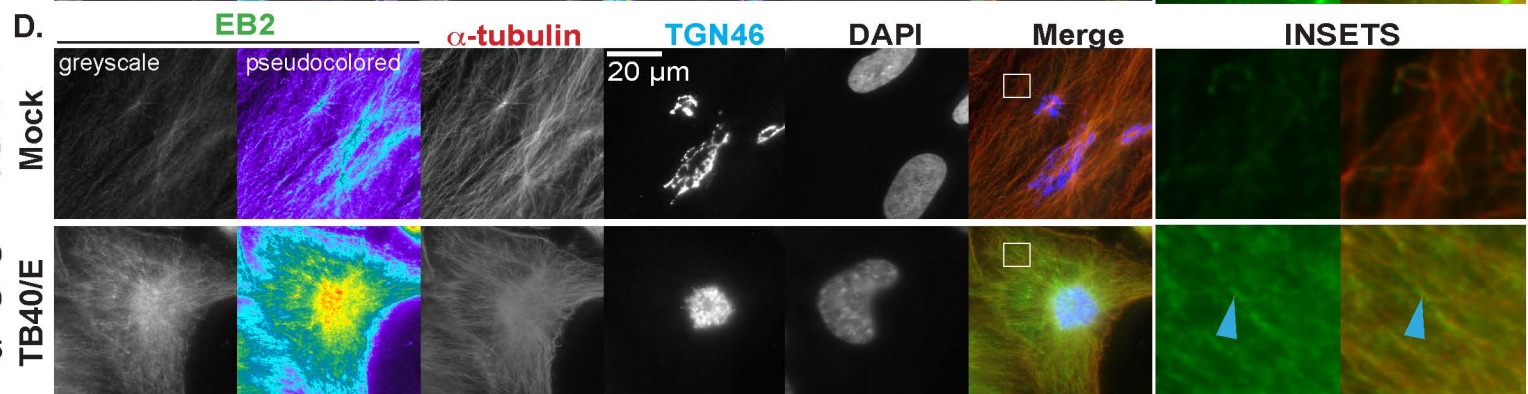
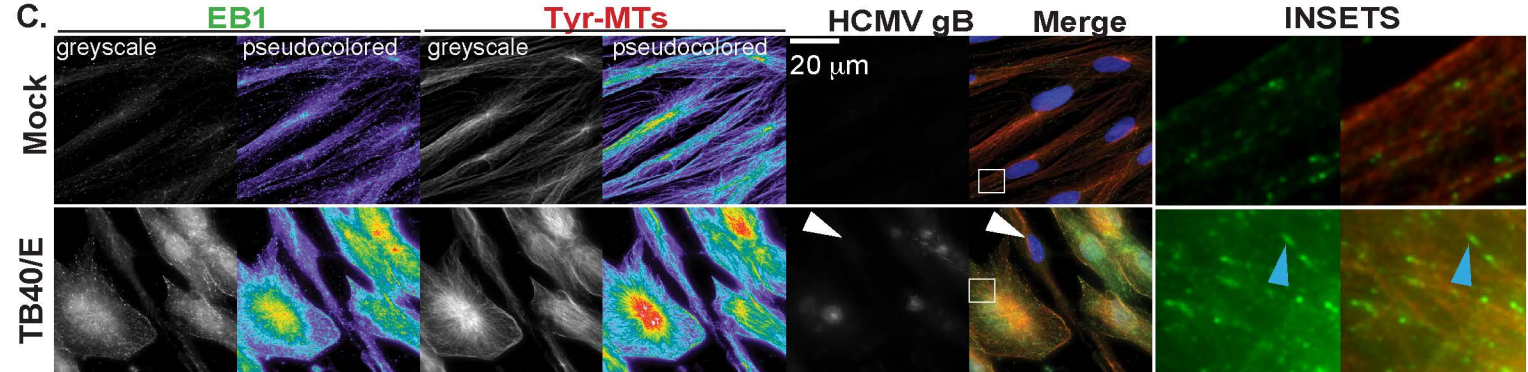
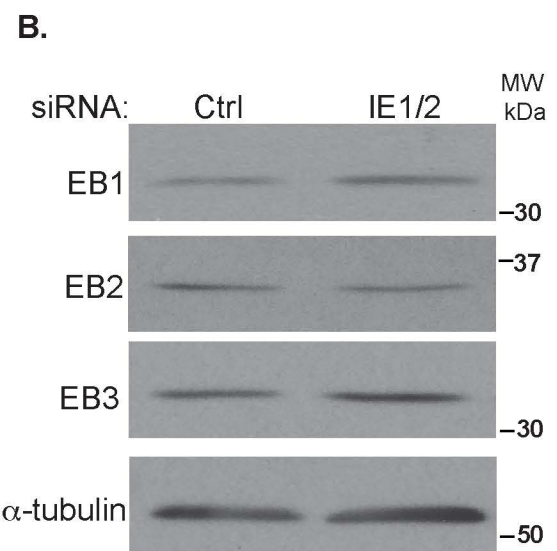
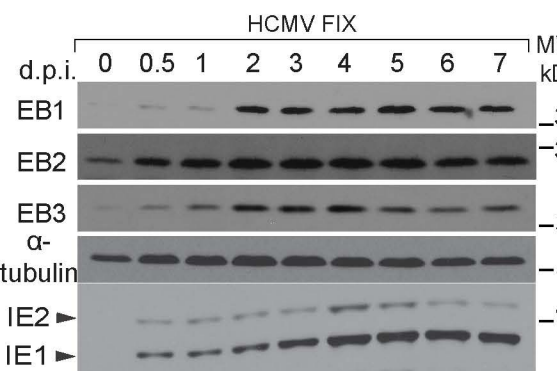
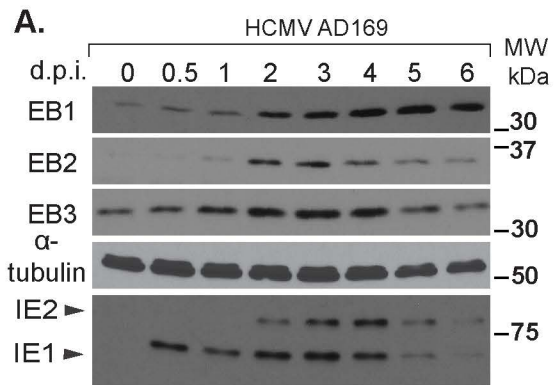
(A) NHDFs were treated with DMSO or 25 μ M HEBTRON and infected with AD169 at MOI 3 for 4d. Fixed samples were stained for EB1, tastin and Hoechst. Zooms show EB1 comets and trailing Tastin on MT plus-ends. (B) Line-scan analysis of EB1 and tastin intensity and distribution in samples in A. Due to antibody incompatibility tastin and EB3 could not be co-stained, and EB1 was used to demark MT plus-ends. The approximate location of EB3 peak intensity (based on separate EB1 and EB3 co-staining; see Figure 5D) corresponds to that of Tastin, suggesting similar localizations of EB3 and Tastin immediately behind EB1. Tastin staining at MT plus-ends is reduced upon HEBTRON treatment. Distributions of EB1 (red) or tastin (green) in DMSO (solid)

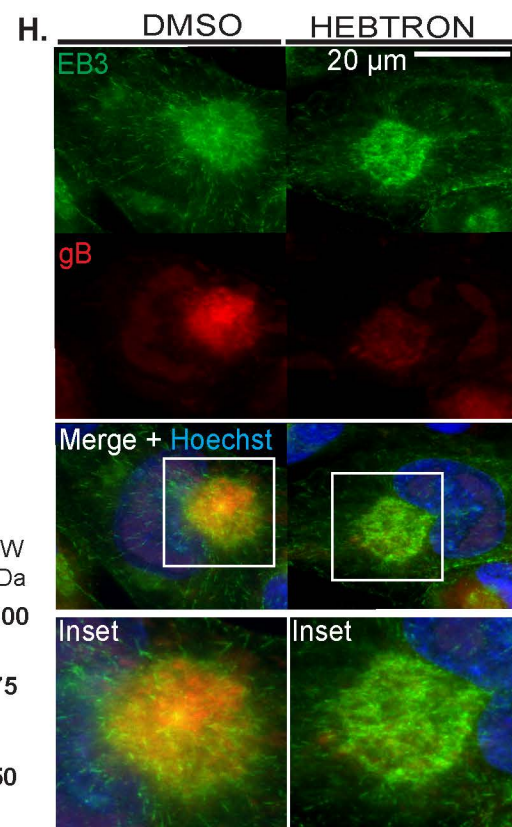
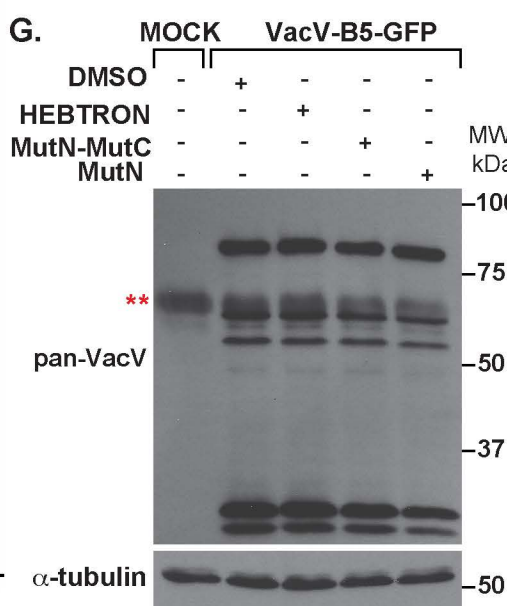
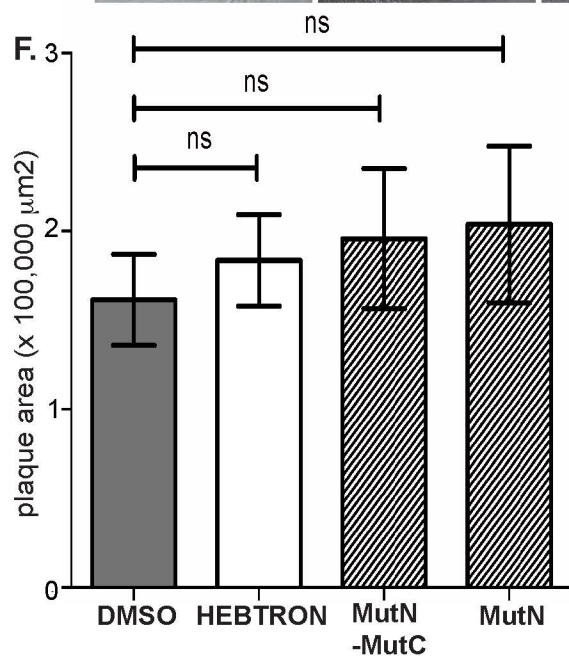
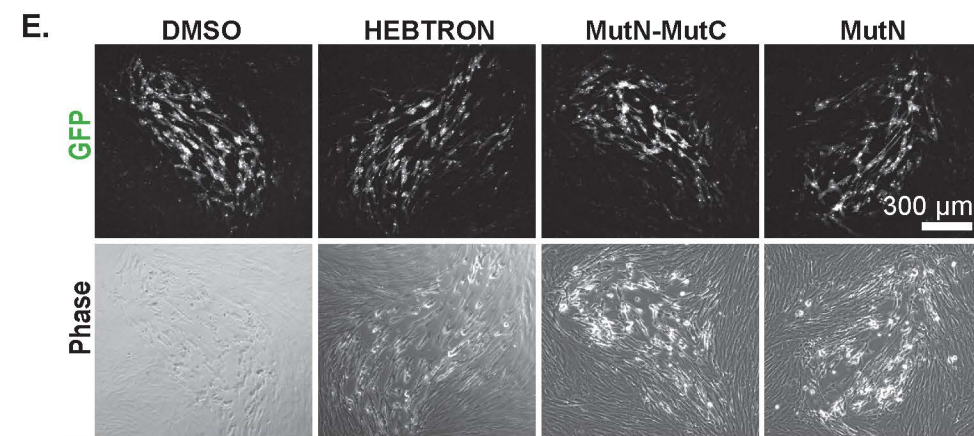
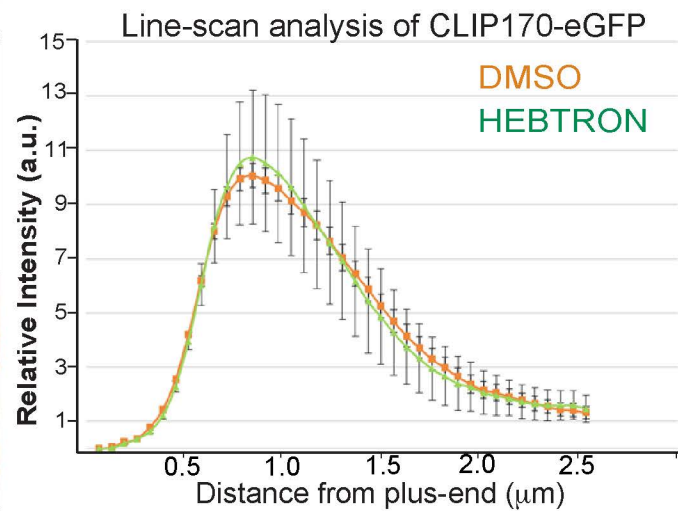
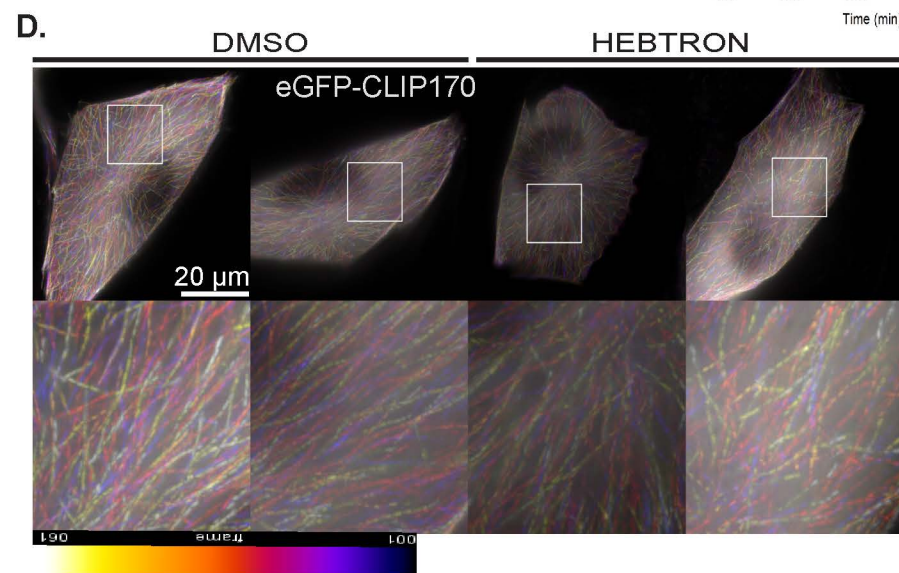
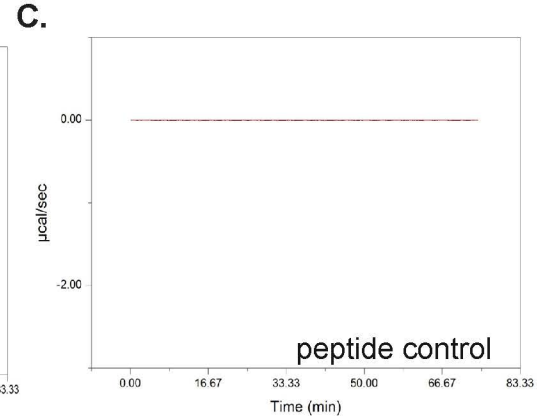
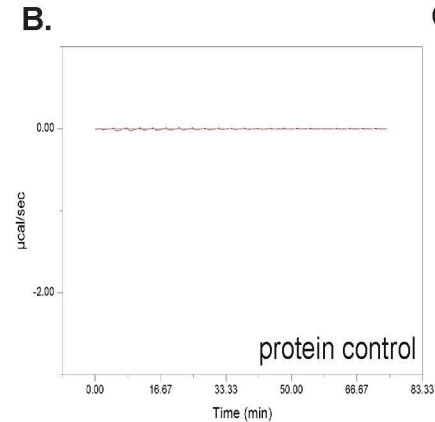
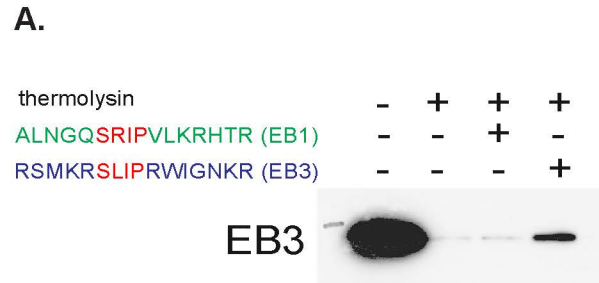
or HEBTRON (dashed) treated samples using MetaMorph. n = 5; bars = s.e.m. (C-D) NHDFs were treated with the indicated siRNAs for 30 h (C) or treated with DMSO or 25 μ M HEBTRON (D) and then infected with AD169 at MOI 3 for 3 d. Cells were then treated with 10 μ M nocodazole for 8h before washout for 0 or 10 min. Samples were stained for TGN46, α -tubulin and acetylated-MTs. White arrows point to examples of TGN46-positive sites that nucleate new acetylated MTs in control samples, or poorly nucleate new MTs in EB3 depleted or HEBTRON-treated cells. The number of new MTs at non-centrosomal sites 10 min post-washout was quantified using Fiji. n = 3 biological replicates, bars = s.e.m., unpaired t-test, **p<0.01, unpaired t-test.

Table S1: Related to Key Resources Table

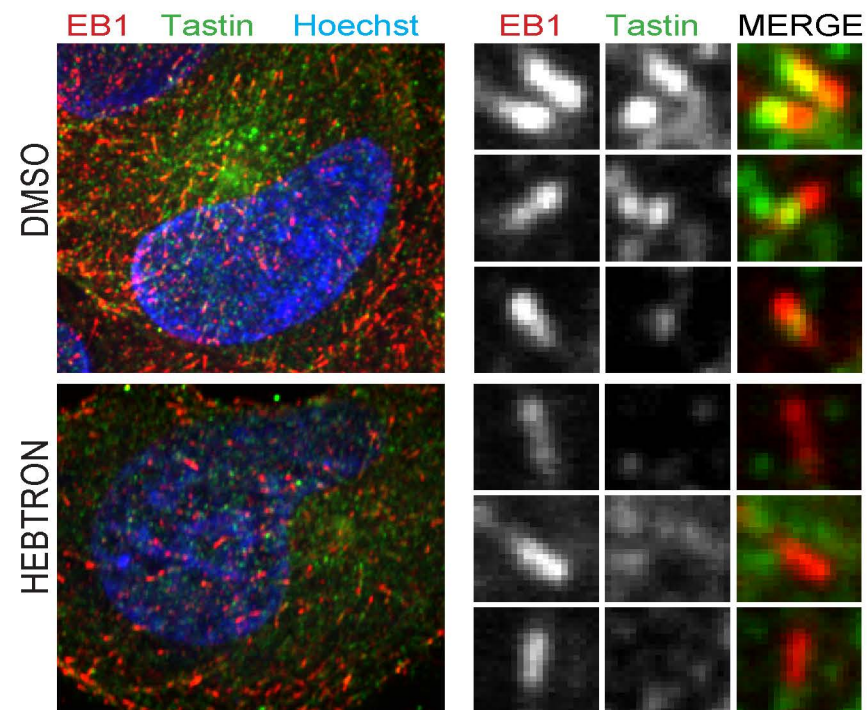
Sequences of siRNAs and primers used in this study.



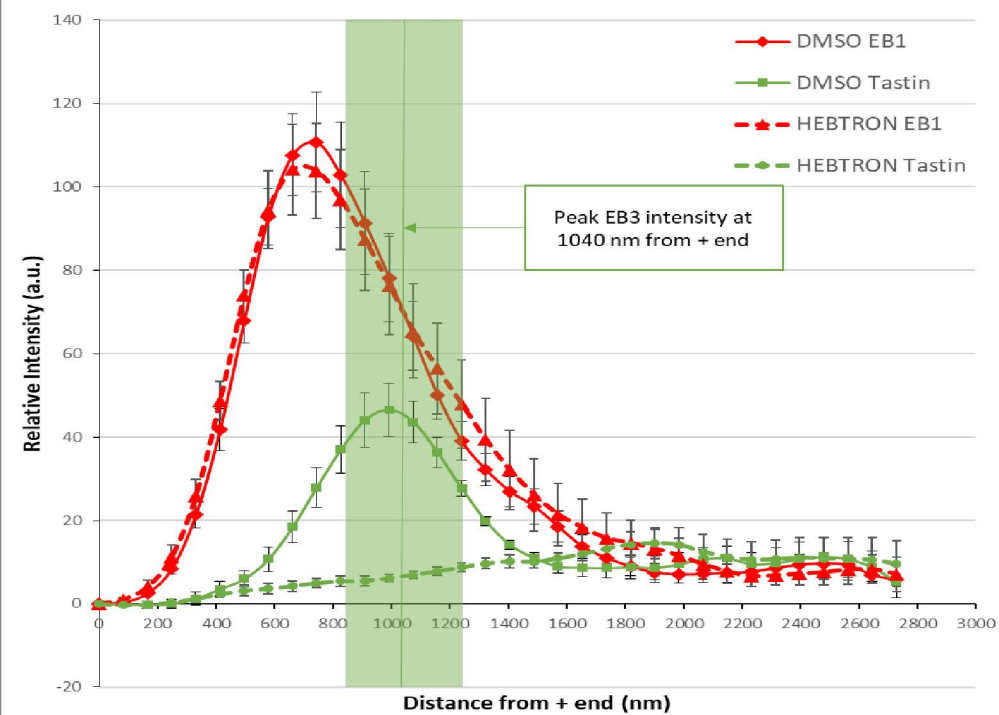




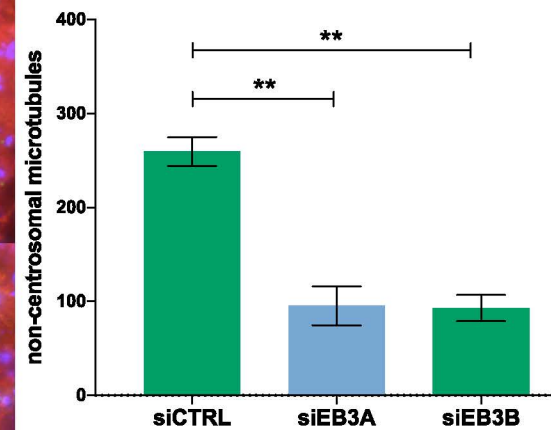
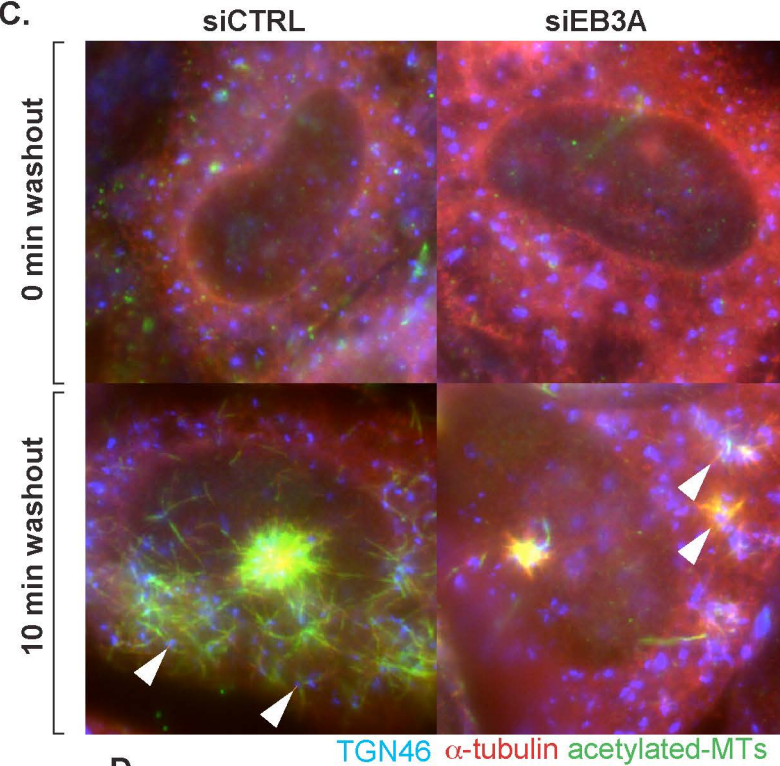
A.



B.



C.



D.

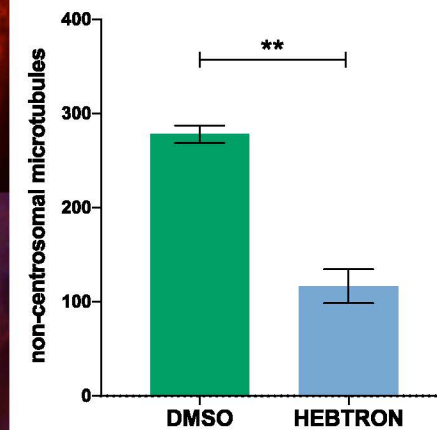
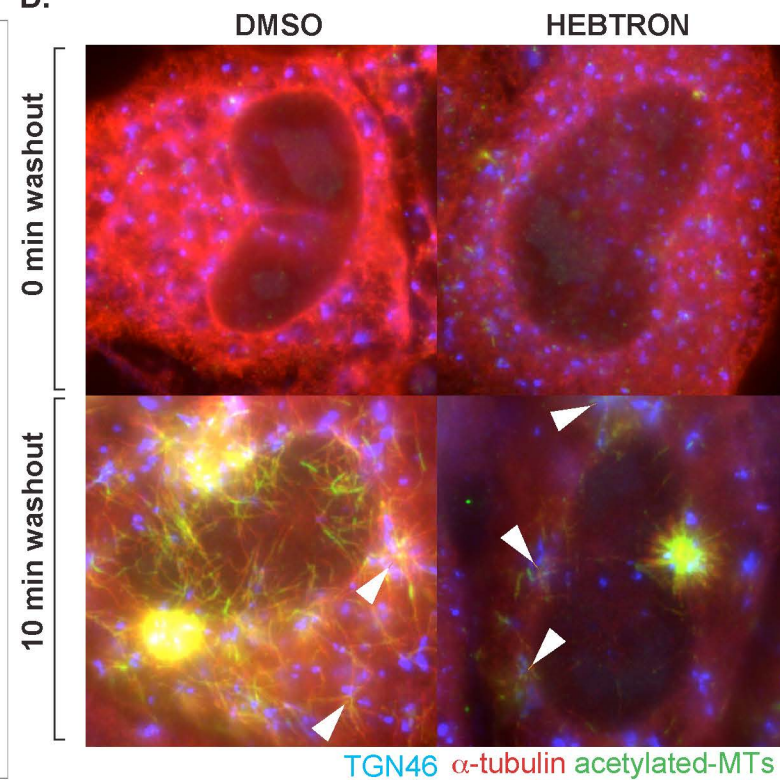


Table S1: Oligonucleotides, related to STAR Methods

REAGENT or RESOURCE	SOURCE	IDENTIFIER
siRNA		
Silencer negative control 1 siRNA (si.CTRL)	Ambion Thermo Fisher Scientific	Cat# AM4635
siRNA targeting EB1-B (si.EB1B)	Ambion Thermo Fisher Scientific	Cat# AM16706 ID#3891
siRNA targeting EB1-C (si.EB1C)	Ambion Thermo Fisher Scientific	Cat# AM16706 ID#136501
siRNA targeting EB3-A (si.EB3A)	Ambion Thermo Fisher Scientific	Cat# AM16704 ID#19984
siRNA targeting EB3-B (si.EB3B)	Ambion Thermo Fisher Scientific	Cat# AM16704 ID#20077
siRNA targeting sequence HCMV-IE1-72: 5'GGUUAUCAGUGUAAUGAAGdTdT-3' and complement 5'CUUCAUUACACUGAUACCCdTdT-3'	Ambion Thermo Fisher Scientific	NA
RT-qPCR primers:		
POLR2L forward primer: 5'-AGGAGAGCCTTCCATCTCG-3'	Tirosh et al 2015	NA
POLR2L reverse primer: 5'-ATCTGGCTCTTCAGATTCCG-3'	Tirosh et al 2015	NA
EB1 forward primer: 5'-CTGTATGCCACAGATGAAGG-3'	Sabo et al 2013	NA
EB1 reverse primer: 5'-CCAGACACAATGTCAAACGC-3'	Sabo et al 2013	NA
EB2 forward primer: 5'-AGAATACACATTGACCGCCA-3'	This paper	NA
EB2 reverse primer: 5'-CAAATGGCGAGAACAACAAC-3'	This paper	NA
EB3 forward primer: 5'-GCCAGAGGTCTGCATGTTTT-3'	This paper	NA
EB3 reverse primer: 5'-GTAGCGCCACCTCCTAACC-3'	This paper	NA
Primers for recombinant DNA construct generation:		
pBABE-puro-AA forward: 5'-ATAGCCGGCACCGGTACATATGGGCCCGGATCCATA-3'	This paper	NA
pBABE-puro-AA reverse: 5'-TATGGATCCGGGCCATATGTACCGGTGCCGGCTAT-3'	This paper	NA
IE1 / IE2 forward: 5'-ATACATATGACCGGTACCATGGAGTCCTCTGCCAAGAGAAAG-3'	This paper	NA
IE1 reverse: 5'-ATACATATGGAATTCTTACTGGTCAGCCTTGCTTCTAG-3'	This paper	NA
IE2 reverse: 5'-ATACATATGGAATTCTTACTGAGACTTGTTCTCAGG-3'	This paper	NA
GFP forward: 5'- ATAGCCGGCCTCGAGATGGTGAGCAAGGGCGA-3'	This paper	NA
GFP reverse: 5'-ATAGAATTCTTACTTGTACAGCTCGTCCATGCCG-3'	This paper	NA
NLS-mCardinal forward: 5'-ATACATATGACCGGTACCATGACTGCTCCAAAGAAGAAGCGTAAGGTAATG GTGAGCAAGGGCGAGGAGCTGATC-3'	This paper	NA

NLS-mCardinal reverse: 5'- TATCATATGGGATCCTTACTTGTACAGCTCGTCCATGCC- 3'	This paper	NA
Oligonucleotides for recombinant virus generation:		
UL99-Galk-5': 5'-CAA CGT CCA CCC ACC CCC GGG ACA AAA AAG CCC GCC GCC CCC TTG TCC TTT CCT GTT GAC AAT TAA TCA TCG GCA	This paper	NA
UL99-Galk-3': 5'-GTG TCC CAT TCC CGA CTC GCG AAT CGT ACG CGA GAC CTG AAA GTT TAT GAG TCA GCA CTG TCC TGC TCC TT-3'	This paper	NA
UL32-Galk-5': 5'-CCG TGC AGA ACA TCC TCC AAA AGA TCG AGA AGA TTA AGA AAA CGG AGG AAC CTG TTG ACA ATT AAT CAT CGG CA-3'	This paper	NA
UL32-Galk-3': 5'-CGT CAC TAT CCG ATG ATT TCA TTA AAA AGT ACG TCT GCG TGT GTG TTT CTT CAG CAC TGT CCT GCT CCT T-3'.	This paper	NA
UL99-eGFP-5': 5'- CAACGTCCACCCACCCCGGGACAAAAAAGCCCGCCGCC CCTTGTCCTTTGTGAGCAAGGGCGAGGAGCTGTTACCG- 3'	This paper	NA
UL99-eGFP-3':5'- GTGTCCCATCCCCGACTCGCGAATCGTACGCGAGACCTGA AAGTTTATGAGTTACTTGTACAGCTCGTCCATGCCGAGAGT -3'	This paper	NA
UL32-Rev-5': 5'-CCG TGC AGA ACA TCC TCC AAA AGA TCG AGA AGA TTA AGA AAA CGG AGG AAA TGG TGA GCA AGG GCG AGG AG-3'	This paper	NA
UL32 Rev-3': 5'-CGT CAC TAT CCG ATG ATT TCA TTA AAA AGT ACG TCT GCG TGT GTG TTT CTT TAC TTG TAC AGC TCG TCC ATG CCG-3'	This paper	NA